# Performance analysis of a graded winding pack design for the EU DEMO TF coil in normal and off-normal conditions

Fusion Engineering and Design 124 (2017) 45–48

Contents lists available at ScienceDirect

Fusion Engineering and Design

journal homepage: www.elsevier.com/locate/fusengdes

# Performance analysis of a graded winding pack design for the EU DEMO TF coil in normal and off-normal conditions

Laura Savoldi[a,*], Alberto Brighenti[a], Roberto Bonifetto[a], Valentina Corato[b], Luigi Muzzi[b,c], Simonetta Turtù[b,c], Roberto Zanino[a]

[a] NEMO Group, Dipartimento Energia, Politecnico di Torino, Italy
[b] ENEA, Frascati, Italy
[c] ICAS, Frascati, Italy

ARTICLE INFO

*Article history:*
Received 3 October 2016
Received in revised form 22 May 2017
Accepted 23 May 2017
Available online 18 August 2017

*Keywords:*
Nuclear fusion
EU DEMO
Superconducting magnets
DC performance
Thermal-hydraulic analysis

ABSTRACT

The superconducting magnet system plays an important role in the framework of the design of the EU DEMO tokamak. In recent years, ENEA developed a prototype of cable-in-conduit conductor (CICC) with two low-impedance central channels to be used in the DEMO Toroidal Field (TF) coils with a graded winding pack (WP). In this paper, a model of a TF coil based on the thermal-hydraulic code 4C has been developed, including the WP, the steel casing with dedicated cooling channels (CCCs) and the two independent cryogenic circuits cooling the WP and the casing, respectively. The first part of the work analyzes the performance of the WP during a series of standard plasma pulses in normal operating conditions. In the second part different off-normal operating conditions during the plasma pulses are studied, namely the collapse of one or both central channel(s) in the most critical CICCs and the plugging of some CCCs at the most critical locations in the magnet.



## 1. Introduction

In the frame of the EU DEMO design activities [1], a big effort is being devoted in the Work Package Magnets (WPMAG) to the preliminary design of the Toroidal Field (TF) coils, resulting in the proposal of three different conductors and corresponding winding packs (WPs) by different European institutions [2,3]. These proposals are periodically updated and optimized taking into account the feedback from mechanical and thermal-hydraulic (TH) analyses, as well as, of course, the updates in the input from the EUROfusion Project Management Unit.

The TH code 4C [4] was already used to develop the first model of an entire EU DEMO TF coil, including structures and a simple cooling circuit [5], and applied, with the addition of quench lines in the model, to the quench analysis of the magnet [6]. In this paper, the previous model is updated to the new WP and conductor designs proposed by ENEA after the 2015 DEMO design review that increased the number of TF coil from 16 to 18 [7]. The model is then used first to assess the coil DC performance, considering, as a major difference with past works analyzing steady state burns [5,8,9], the standard pulsed operation currently foreseen for DEMO: several cycles are simulated, up to a periodic behavior of the coil. The value (and location) of the minimum temperature margin ($\Delta T^{min}_{marg}$) in the WP is computed and compared with the minimum acceptable value of 1.5 K [2]. The study is then repeated in off-normal conditions, i.e. considering the choking of the flow in the pressure relief channels of the most critical conductor or in some casing cooling channels (CCCs).

## 2. Conductor and WP

The most recent WP proposal by ENEA (the so-called WP2016#2) is an upgrade of the 2015 design [10] and consists of a double-layer (DL) wound WP, see Fig. 1a, that allows the grading of the SC cross section in the different DLs, depending on the magnetic field, thus optimizing the use of SC. The WP consists of six DLs where the jacket thickness of each conductor increases with the distance from the plasma to withstand the higher mechanical stresses [11]. The originally circular cable-in-conduit conductors (CICCs) are compacted and squeezed to a rectangular shape, see Fig. 1b, with two low-impedance cooling channels ("holes") [10] delimited by spirals.

Each DL is constituted by a single conductor; the supercritical He at the nominal conditions of 4.5 K and 0.6 MPa is supplied to

* Corresponding author.
*E-mail address:* laura.savoldi@polito.it (L. Savoldi).

http://dx.doi.org/10.1016/j.fusengdes.2017.05.107

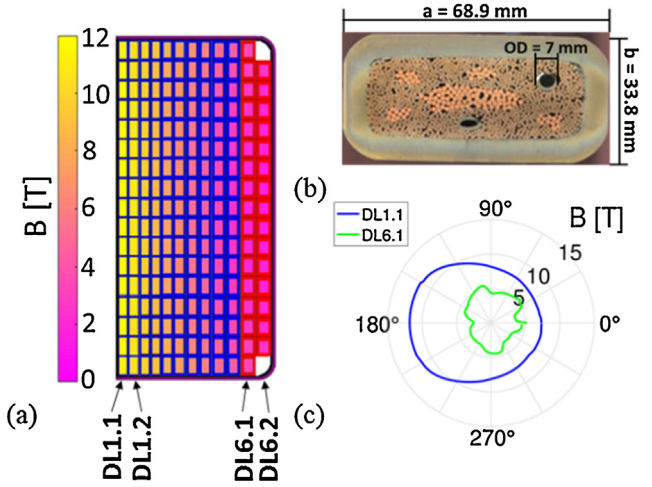


**Fig. 1.** (a) ENEA 2016 design of the TF WP with six DLs including $Nb_3Sn$ (blue) and NbTi (red) conductors. The 2D magnetic field amplitude map on the inboard equatorial cross section is reported (the plasma is on the left). (b) Cross section of the ENEA conductor concept on which 2016 WP design is based. (c) Polar distribution of the magnetic field amplitude in the central turn of DL1.1 (blue) and in the last turn of DL6.1 (green), at nominal operating current; the inboard equatorial plane is at 180°. (For interpretation of the references to colour in this figure legend, the reader is referred to the web version of this article.)

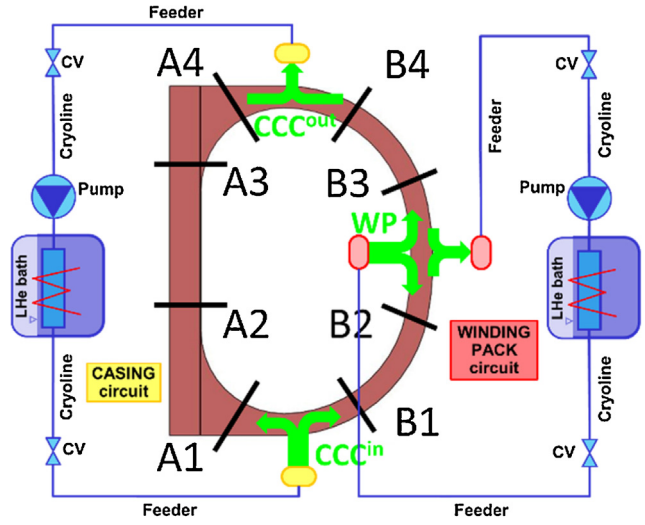


**Fig. 2.** Schematic representation of the 4C model of the cryogenics circuits for WP (on the right, red manifolds) and CCCs (on the left, yellow manifolds) of the DEMO TF coil. The poloidal cuts A1-4, B1-4 used for the discretization of the casing are highlighted. (For interpretation of the references to colour in this figure legend, the reader is referred to the web version of this article.)

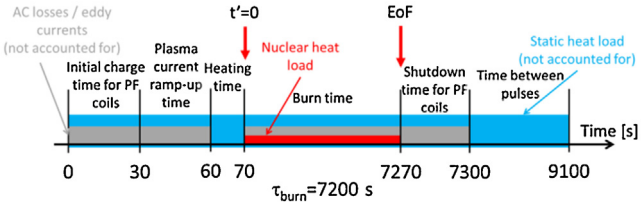


**Fig. 3.** Evolution of a standard DEMO plasma pulse according to [15].

the two layers of the same DL through a single inlet (a hole in the jacket). The inlet mass flow splits between the two layers, so that the He flows in counter-current in adjacent layers. In each layer, the He distributes among the three parallel cooling channels (i.e. the two holes and the bundle) according to their hydraulic impedance. The main geometrical parameters of the conductors are reported in Table 1.

## 3. The 4C model of the TF coil

The 4C model adopted here includes, as in [5], all DLs of the WP (see [12] for details), and the casing, thermally coupled to the WP across the ground insulation and cooled by dedicated CCCs. The casing is discretized in eight poloidal cuts, equally spaced on the inboard (A1-A4) and outboard (B1-B4) legs, see Fig. 2.

The He inlets are located on the equatorial plane of the outboard leg, on the lateral side of the WP, while the outlets are located on the opposite side, at the same poloidal location. The CCCs inlets are located at the bottom of the coil, as in ITER [13]. Each of the two legs has 48 CCCs connected to inlet/outlet manifolds. We consider here the once-through circulation option [5]. The preliminary design of two cryogenic circuits for the WP and for the casing cooling of [5] is adopted, see Fig. 2, supplying ~150 g/s to the CCCs circuit and ~60 g/s to the WP (with the target pressure drop of ~1 bar and inlet pressure of ~6 bar during the transient [14]).

The distribution of the magnetic field at End of Flat top (EoF, see below) and nominal operating current (70.8 kA) is reported in Fig. 1a and c, including all contributions from the Central Solenoid (CS), the Poloidal Field (PF) coils and the plasma. The highest field within the WP is located on the central turns of DL1.1, the innermost layer, at the inboard equatorial plane, while on the outermost DLs the maximum magnetic field is located at the coil sides due to PF contribution, see Fig. 1a and c.

## 4. Simulation setup

The nominal pulsed operation ("normal" operation, case α) consists in a series of standard cycles [15], see Fig. 3, including a 7200 s

**Table 1**
Main geometrical parameters EU DEMO TF WP2016 by ENEA. Where different, the values for the first and second layer of the same DL are separated by "/".

| | $Nb_3Sn$ | | | | | NbTi |
|---|---|---|---|---|---|---|
| | DL1 | DL2 | DL3 | DL4 | DL5 | DL6 |
| N. SC strands (D = 1 mm) | 720 | 360 | 270 | 180 | 120 | 972 |
| Strand Cu:nonCu | 1 | 1 | 1 | 1 | 1 | 1.6 |
| N. Cu strand (D = 1 mm) | 360 | 720 | 540 | 630 | 960 | 0 |
| N. Cu strand (D = 1.5 mm) | 108 | 54 | 162 | 108 | 0 | 108 |
| ID (OD) central channels [mm] | 5 (7) | 5 (7) | 5 (7) | 5 (7) | 5 (7) | 5 (7) |
| Bundle void fraction [%] | 0.26 | 0.26 | 0.26 | 0.26 | 0.26 | 0.3 |
| Jacket ext. dimensions a × b [mm] | 68.9 × 33.8 | 68.9 × 34.9 | 68.9 × 38.6 | 68.9 × 40.8 | 68.9 × 46.2 | 68.9 × 56.6 |
| Jacket thickness [mm] | 3.9 | 5.3 | 6.8 | 8.4 | 10.0 | 11.7 |
| Turn length [m] | 43.92/44.16 | 44.40/44.64 | 44.90/45.17 | 45.44/45.72 | 46.02/46.34 | 46.68/47.06 |
| # turns | 17/17 | 17/17 | 17/17 | 17/17 | 17/17 | 17/15 |
| Hydraulic length [m] | 746/751 | 755/759 | 763/768 | 772/777 | 782/788 | 794/706 |

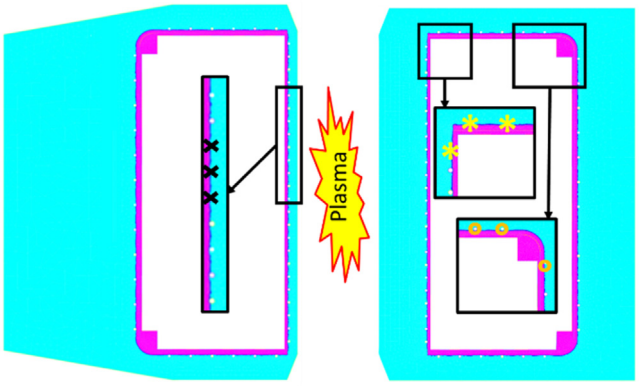


**Fig. 4.** The CCCs design is shown for both inboard (left) and outboard (right) legs of the coil. Plugged channels are highlighted with crosses for case δ, stars for case ζ and circles for case η.

plasma burn and ~1800s dwell time, which are simulated here until periodicity is reached.

Only the nuclear heat (NH) load $P_{NH}(r) = 50\exp\left(-r/140\right)$ [W/m$^3$] is accounted for in both casing and WP in the current analysis, as a function of the radial distance $r$ (in mm) from the plasma facing wall [16], while more detailed NH maps based on Monte Carlo calculations are being prepared and will be implemented in future analyses. The static heat load on the casing surface and the AC/eddy current losses in the conductor/casing during CS and PF coils current ramps are not accounted for.

We then consider also the pulsed operation when the cooling capability in a subset of cooling paths is reduced ("off-normal" operation), and namely the flow is choked:

- in the relief channels of the CICCs with the lowest $\Delta T_{marg}$ (DL1.1, DL1.2 and DL6.1), corresponding e.g. to the collapse of one (case β) or both (case γ) spirals, due to the high mechanical stress during the conductor compaction
- in the most critical CCCs, corresponding to the plugging of some CCCs in proximity of the $\Delta\, T^{\min}_{marg}$ location in DL1.1 (facing the casing all along its length, case δ), near the outlet of DL2.1 ($\Delta\, T^{\min}_{marg}$ for $Nb_3Sn$ DLs, case ζ) and near the outlet of DL6.1 (absolute $\Delta\, T^{\min}_{marg}$ location, case η), see Fig. 4 – a situation that is relevant since the CCCs play an important role in the removal of the NH load, partially contributing also to the cooling of the WP [5].

## 5. Results

### 5.1. Normal operation

The periodic behavior in normal operation is reached after two cycles, as shown in Fig. 5a, reporting the evolution of both the maximum cable temperature and $\Delta\, T^{\min}_{marg}$ in DL1.1 (the most loaded conductor). At EoF the $\Delta\, T^{\min}_{marg}$ requirement of 1.5 K is satisfied in all the conductors, see Fig. 5b. Only in DL6.1 (NbTi) it is slightly below the threshold, ~1.43 K, but this is well within the uncertainty on the NH load used in input. In Fig. 5b it is also shown that, with respect to the initial steady state value, the NH during cyclic operation erodes the initial available $\Delta\, T^{\min}_{marg}$ of ~0.1 ÷ 0.4 K, depending on the distance from the plasma. Note, however, that the adiabatic condition assumed for the casing surface is not conservative, so that any design for the casing cooling should also be addressed to the static load removal, once a good estimate of it will become available, not to affect and reduce the $\Delta\, T^{\min}_{marg}$.

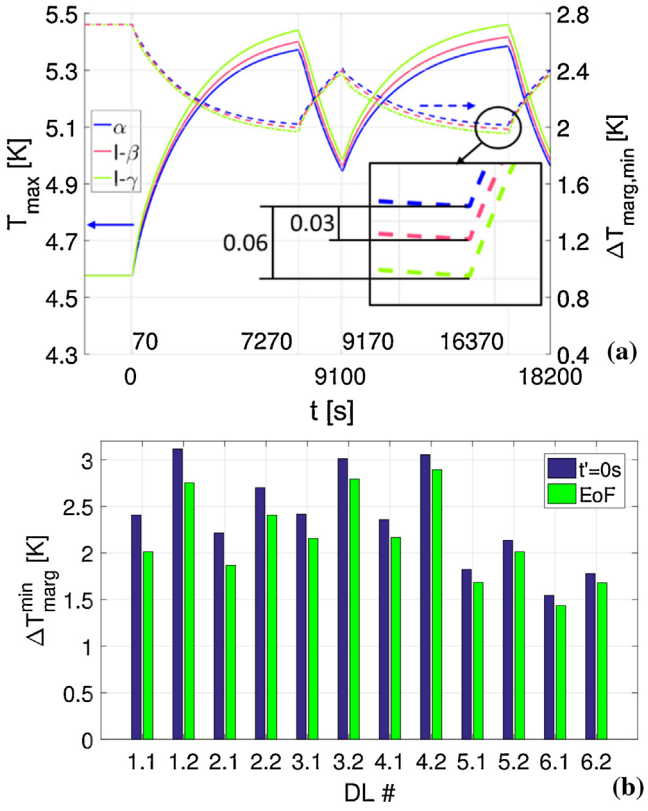


**Fig. 5.** (a) Evolution of the maximum cable temperature (solid lines, left axis) and of the $\Delta\, T^{\min}_{marg}$ (dashed lines, right axis) for case α (blue), β (pink) and γ (green) during the first two cycles, for DL1.1 (case I). (b) $\Delta\, T^{\min}_{marg}$ in all layers before the plasma burn start at $t'$=0 s (blue bars), see also Fig. 3, and at EoF of a periodic pulse (green bars). (For interpretation of the references to colour in this figure legend, the reader is referred to the web version of this article.)

### 5.2. Off-normal operation

The evolution of the $\Delta T_{marg}$ at EoF during the standard plasma burn for both cases I-β and I-γ are reported in Fig. 5a, where it is compared with the nominal case α, showing that a maximum $\Delta T_{marg}$ reduction <0.1 K is computed, see also Table 2, in the worst case (γ), despite a reduction of the mass flow rate >50%. The decrease of the active cooling of the WP is indeed compensated by an increase of the heat transfer to the casing in case of DL1.1, see Fig. 6, and/or to the neighboring layers.

The effect of CCCs plug on the $\Delta\, T^{\min}_{marg}$ in the different cases is also always <0.1 K, as summarized in Table 2.

**Table 2**
Summary of the $\Delta\, T^{\min}_{marg}$ erosion at EoF in the different off-normal operating conditions.

| | Case | Temperature margin erosion | |
|---|---|---|---|
| | | $\Delta(\Delta T_{marg})$ [K] | [%] |
| DL1.1 | β | −0.03 | −1.4 |
| | γ | −0.06 | −3.0 |
| DL2.1 | β | −0.02 | −1.1 |
| | γ | −0.04 | −1.9 |
| DL6.1 | β | −0.01 | −0.5 |
| | γ | −0.01 | −0.7 |
| CCC | δ | −0.08 | −3.8 |
| | ζ | −0.04 | −1.9 |
| | η | −0.02 | −1.5 |

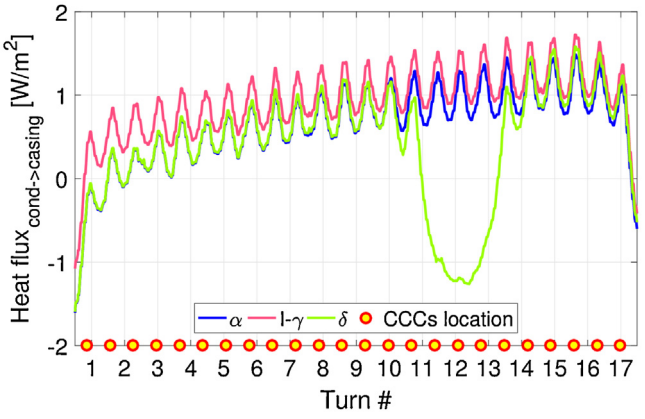


**Fig. 6.** Heat flux from conductor to casing at cut A3, corresponding to the $\Delta T^{\min}_{\text{marg}}$ location on DL1.1, for cases α (blue), I-γ (pink) and δ (green). (For interpretation of the references to colour in this figure legend, the reader is referred to the web version of this article.)

The DL1.1 is, as expected, the most affected by the cooling reduction caused by the CCCs plugging, since it is in contact with the casing all along its length: Fig. 6 shows the negative heat transfer from the WP to the casing (i.e., the WP is heated by the casing) in correspondence of the plugged CCCs, close to turn #12, for case δ. This is however a conservative situation, as the detachment of the WP from the plasma side of the casing during burn is not taken into account.

## 6. Conclusions and perspective

The 4C model of an EU DEMO TF coil has been applied to assess the coil performance during standard pulsed operation. The computed $\Delta T^{\min}_{\text{marg}}$ is in line with the design value of 1.5 K assuming the static heat load on the casing surface is negligible. As soon as a good estimate of it will become available, we plan to include it in the analysis and the design of the casing cooling should then be targeted to remove it, not to decrease the WP temperature margin.

Off-normal operating conditions, including the reduction of the available cooling due to collapse of relief channels in the WP and plugging of selected CCCs at critical locations, have also been analyzed, showing that the corresponding erosion of the $\Delta T_{\text{marg}}$ remains in all cases marginal (<0.1 K).

## Acknowledgments

This work has been carried out within the framework of the EUROfusion Consortium and has received funding from the Euratom research and training programme 2014–2018 under grant agreement No 633053. The views and opinions expressed herein do not necessarily reflect those of the European Commission.

## References

[1] F. Romanelli, et al., Fusion Electricity. A Roadmap to the Realisation of Fusion Energy [Online], 2016, Available: https://www.euro-fusion.org/wpcms/wp-content/uploads/2013/01/JG12.356-web.pdf. (Accessed on 31 July 2016).
[2] L. Zani, et al., Overview of progress on the EU DEMO magnet system design, IEEE Trans. Appl. Supercond. 26 (4) (2016) 4204505.
[3] L. Zani, et al., Overview of Pre-conceptual Design Activities on EU DEMO Reactor Magnet System, presented at ASC 2016 and to be submitted to IEEE Transactions on Applied Superconductivity.
[4] L. Savoldi Richard, F. Casella, B. Fiori, R. Zanino, The 4C code for the cryogenic circuit conductor and coil modeling in ITER, Cryogenics 50 (2010) 167–176.
[5] R. Zanino, et al., Development of a thermal-Hydraulic model for the european DEMO TF coil, IEEE Trans. Appl. Supercond. 26 (3) (2016) 4201606.
[6] L. Savoldi, et al., Quench propagation in a TF coil of the EU DEMO, to appear in Fusion Science and Technology (2017).
[7] F. Nunio, TF Magnet system configuration from IDM central database CAD model, EFDA_D_2LMDTE, 04/06/2015, unpublished document.
[8] M. Lewandowska, K. Sedlak, L. Zani, Thermal-Hydraulic analysis of the low-$T_c$ superconductor (LTS) winding pack design concepts for the DEMO toroidal field (TF) coil, IEEE Trans. Appl. Supercond. 26 (4) (2016) 4205305.
[9] R. Vallcorba, et al., Thermo-hydraulic analyses associated with a CEA design proposal for a DEMO TF conductor, Cryogenics 80 (3) (2016) 317–324.
[10] L. Muzzi, et al., Design, manufacture and test of an 80 kA-class Nb3Sn cable-in-conduit conductor with rectangular geometry and distributed pressure relief channels, IEEE Trans. Appl. Supercond. 27 (4) (2017) 4800206.
[11] A. Panin, et al., Approaches to analyze structural issues of the european DEMO toroidal field coil system at an early design stage, IEEE Trans. Appl. Supercond. 26 (4) (2016), Art. ID 4200805.
[12] L. Savoldi, R. Bonifetto, L. Muzzi, R. Zanino, Analyses of low- and high-margin quench propagation in the european DEMO TF coil winding pack, IEEE Trans. Plasma Sci. 44 (9) (2016) 1564–1570.
[13] L. Savoldi Richard, et al., Mitigation of the temperature margin reduction due to the nuclear radiation on the ITER TF coils, IEEE Trans. Appl. Supercond. 23 (3) (2013) 4201305.
[14] M. Lewandowska, K. Sedlak, L. Zani, Thermal-hydraulic analysis of the low Tc superconductor (LTS) winding pack design concepts for the DEMO toroidal field (TF) coil, IEEE Trans. Appl. Supercond. 26 (4) (2016), 4205305.
[15] B. Meszaros, EU DEMO1 2015 Plasma and equilibrium description, EFDA_D_2LJFN7, 18/05/2015, unpublished document.
[16] L. Zani and U. Fischer, Advanced definition of neutronic heat load density map on DEMO TF coils, EFDA_D_2MFVCA, 18/10/2014, unpublished document.